Mechanism of Transfer of the Methyl Group from (6*S*)-Methyltetrahydrofolate to the Corrinoid/Iron−Sulfur Protein Catalyzed by the Methyltransferase from *Clostridium thermoaceticum*: A Key Step in the Wood−Ljungdahl Pathway of Acetyl-CoA Synthesis†

Javier Seravalli, Shaying Zhao,‡ and Stephen W. Ragsdale*

Department of Biochemistry, Beadle Center, City Campus, University of Nebraska, Lincoln, Nebraska 68588-0664

Received October 16, 1998; Revised Manuscript Received February 17, 1999

ABSTRACT: The methyltetrahydrofolate:corrinoid/iron−sulfur protein methyltransferase (MeTr) from *Clostridium thermoaceticum* catalyzes transfer of the N^5-methyl group from (6*S*)-methyltetrahydrofolate (CH_3-H_4folate) to the cobalt center of a corrinoid/iron−sulfur protein (CFeSP), forming methylcob(III)amide and H_4folate. This reaction initiates the unusual biological organometallic reaction sequence that constitutes the Wood−Ljungdahl or reductive acetyl-CoA pathway. The present paper describes the use of steady-state, product inhibition, single-turnover, and kinetic simulation experiments to elucidate the mechanism of the MeTr-catalyzed reaction. These experiments complement those presented in the companion paper in which binding and protonation of CH_3-H_4folate are studied by spectroscopic methods [Seravalli, J., Shoemaker, R. K., Sudbeck, M. J., and Ragsdale, S. W. (1999) *Biochemistry 38,* 5736−5745]. Our results indicate that a pH-dependent conformational change is required for methyl transfer in the forward and reverse directions; however, this step is not rate-limiting. CH_3-H_4folate and the CFeSP [in the cob(I)amide state] bind randomly and independently to form a ternary complex. Kinetic simulation studies indicate that CH_3-H_4folate binds to MeTr in the unprotonated form and then undergoes rapid protonation. This protonation enhances the electrophilicity of the methyl group, in agreement with a 10-fold increase in the pK_a at N^5 of CH_3-H_4folate. Next, the Co(I)-CFeSP attacks the methyl group in a rate-limiting S_N2 reaction to form methylcob(III)amide. Finally, the products randomly dissociate. The following steady-state constants were obtained: $k_{cat} = 14.7 \pm 1.7\ s^{-1}$, K_m of the CFeSP $= 12 \pm 4\ \mu M$, and K_m of (6*S*)-CH_3-H_4folate $= 2.0 \pm 0.3\ \mu M$. We assigned the rate constants for the elementary reaction steps by performing steady-state and pre-steady-state kinetic studies at different pH values and by kinetic simulations.

Clostridium thermoaceticum and other anaerobic bacteria fix CO or CO_2 by the Wood−Ljungdahl pathway of acetyl-CoA synthesis (*1*−*3*). This pathway also is responsible for the ability of acetogenic bacteria to synthesize 3, instead of 2, mol of acetyl-CoA per mole of glucose. A unique feature of the Wood−Ljungdahl pathway is that it involves a series of enzyme-bound organometallic intermediates. The first intermediate in this biological organometallic reaction sequence is a methylcobalt species, which is formed by transfer of the N^5-methyl group from (6*S*)-CH_3-H_4folate[1] to the cobalt center of a corrinoid iron−sulfur protein (CFeSP) (eq 1). This reaction, which is the focus of the present paper, is catalyzed by a methyltetrahydrofolate:corrinoid/iron−sulfur protein methyltransferase (MeTr). Subsequent steps in the pathway involve transfer of the methyl group to an enzyme called CO dehydrogenase/acetyl-CoA synthase (CODH/ACS) where it combines with CoA and carbon monoxide to generate acetyl-CoA.

$$CH_3\text{-}H_4\text{folate} + \text{cob(I)amide} \rightleftharpoons H_4\text{folate} + CH_3\text{-cob(III)amide} \quad (1)$$

MeTr has been purified to homogeneity (*4*) and crystallized (*5*). The protein lacks metals or other prosthetic groups, and is one of the few oxygen-stable proteins in the Wood−Ljungdahl pathway (*6*). MeTr has a homodimeric structure with two 28 kDa subunits (*4, 6*). The corresponding gene has been cloned, sequenced, and actively overexpressed in *Escherichia coli* (*7, 6*). Location of the H_4folate binding domain has been accomplished by observing significant sequence homology with a region adjacent to the cobalamin binding site of methionine synthase (*6*).

The physiological acceptor of the methyl group of CH_3-H_4folate is the CFeSP, an 88 kDa heterodimeric protein with subunit molecular masses of 33 and 55 kDa (*8, 9*). The 55 kDa subunit contains a $[4Fe\text{-}4S]^{2+/1+}$ cluster that is involved in reductive activation of the cobalt center (*10*). The cobalt center, 5′-methoxybenzimidazolylcobamide, is bound pre-

† This work was supported by NIH Grant GM39451 (S.W.R.).

* Correspondence should be addressed to this author. Phone: 402-472-2943. Facsimile: 402-472-7842. Internet: sragsdal@unlinfo.unl.edu.

‡ Present address: The Institute for Genomic Research, 9712 Medical Center Dr., Rockville, MD 20850.

[1] Abbreviations: CH_3-B_{12}, methylcobalamin; CH_3-H_4folate, methyltetrahydrofolate; CFeSP, corrinoid/iron−sulfur protein; MeTr, methyltetrahydrofolate:corrinoid/iron−sulfur protein methyltransferase; CODH/ACS, CO dehydrogenase/acetyl-CoA synthase; SHE, standard hydrogen electrode; PCA, protocatechuic acid; PCD, protocatechuate dioxgenase; MES, 2-(*N*-morpholino)ethanesulfonate.

10.1021/bi982473c CCC: $18.00
Published on Web 04/15/1999

dominantly to the 33 kDa subunit (*9, 11*). Stopped-flow studies have shown that the methyl transfer reaction involves a nucleophilic attack by the Co(I) state of the CFeSP on the methyl group of (6*S*)-CH_3-H_4folate (*12*). Thus, during catalysis, the CFeSP cycles between the cob(I)amide and methylcob(III)amide states. In approximately 1 in 100 turnovers, cob(I)amide escapes from the catalytic cycle by oxidation to cob(II)amide (*13*). Then, reductive activation is required to regenerate cob(I)amide. These features of the catalytic mechanism are reminiscent of those of the cobalamin-dependent methionine synthase, which, however, has a more complicated reductive activation mechanism involving adenosylmethionine (*14*). Changes in coordination chemistry—removing the lower axial cobalt ligand and imposing other subtle electronic changes on the cobalt center—enhance the methyl transfer properties of the CFeSP (*9, 15*−*17*).

The focus of the studies described in this paper was to elucidate the kinetic mechanism of the MeTr reaction. It has been proposed that protonation of the N^5 or C^{8a} group of CH_3-H_4folate could facilitate the methyl transfer reaction by making the bound methyl group more electrophilic and, hence, more subject to the nucleophilic attack by cob(I)amide (*18, 19*). The rate of the MeTr reaction increases as the pH is lowered ($pK_a \sim 5.0$) (*12*), following a pH profile that is similar to that observed for ionization of the N^5 group of (6*S*)-CH_3-H_4folate. Protonation of MeTr-bound CH_3-H_4folate has been recently demonstrated by NMR studies (*20*). However, a conformational change in MeTr, not substrate protonation, appears to be responsible for the pH dependence of the reaction (*21*).

The results described in this paper include single-turnover, initial velocity, product inhibition, and kinetic simulation experiments that have allowed us to describe and assign rate constants for the elementary steps in the MeTr-catalyzed reaction. Overall, the reaction was defined as a random Bi-Bi mechanism, and the methyl transfer step is rate-limiting.

MATERIALS AND METHODS

Materials. (6*S*)-CH_3-H_4folate was a generous gift from SAPEC S.A. in Switzerland. (6*S*, 6*R*)-H_4folate was purchased from Dr. B. Schircks Laboratories in Switzerland. $Ti^{III}Cl_3$ was purchased from Aldrich. Methylcobalamin (CH_3-B_{12}) and protocatechuic acid (PCA) were purchased from Sigma. Protocatechuate dioxygenase (PCD) was a generous gift from Dr. David P. Ballou (The University of Michigan) and Dr. John Lipscomb (The University of Minnesota). Other reagents were of analytical grade from either Sigma or Aldrich and were used without further purification.

Enzyme Preparation. C. thermoaceticum was grown as described (*22*). All proteins were purified at 18 °C under strictly anaerobic conditions in either a Vacuum Atmospheres or a Coy Laboratory Products anaerobic chamber. The CFeSP (*9*), MeTr (*8*), ferredoxin II (FdII) (*23*), and CODH/ACS (*24*) were purified to homogeneity as described. A CFeSP stock solution was desalted using an Amicon Mirocon concentrator (Model 30) by washing with 3 volumes of 1 mM Tris-HCl, pH 7.6, containing 0.1 M NaCl. The concentration of protein was determined by the Rose Bengal method (*25*).

Determination of k_{cat} and k_{cat}/K_m for the CFeSP. Steady-state experiments were performed on a modified Cary-14 spectrophotometer (On-Line Instrument Systems Inc.) at 25 °C. The temperature of the reaction was controlled by a circulating water bath. For initial rate studies, the concentration of (6*RS*)-CH_3-H_4folate was fixed at 58 μM and the CFeSP concentration was varied. The CFeSP was reduced to the cob(I)amide state by the procedure described above. The initial velocity was calculated based on a difference extinction coefficient ($\Delta\epsilon$) between cob(I)amide and methylcob(III)amide of 17 mM^{-1} cm^{-1} (*12*). Values of k_{cat} and k_{cat}/K_m for CFeSP were calculated from the dependence of initial rates on CFeSP concentration at each pH as shown in Figure 1. The steady-state traces at several pH values, which were used for simulations, were obtained in a 2 mm cell path at 390 nm at constant concentrations of 70 μM (6*RS*)-CH_3-H_4folate, 74 μM CFeSP, 31 nM MeTr, and 50 mM MES buffer at an ionic strength of 0.1. Other conditions are provided in the Figure 4A legend.

Product Inhibition Studies. The CFeSP was methylated as previously described (*12*). All solutions were made anaerobic either by bubbling with N_2 or by preparing in the anaerobic chamber. The cuvettes with red-rubber stoppers, and a cell path of 1 or 0.2 cm, were placed in a Schlenk line, and the atmosphere was exchanged by flushing with nitrogen for 20 min. In one set of experiments, the concentration of CFeSP was fixed at 20 μM and the concentrations of (6*S*)-CH_3-H_4folate (the substrate) and either H_4folate or CH_3-CFeSP (the product inhibitors) were varied. In another set of experiments, (6*S*)-CH_3-H_4folate was fixed at either saturating (50 μM) or unsaturating (0.8 μM) concentrations and the CFeSP concentration was varied in the presence of one of the products. The CFeSP was reduced by Ti(III) citrate. The initial velocity was obtained by monitoring the absorbance decrease at 390 nm.

Single-Turnover Studies of the Methylation of the CFeSP. The study of the forward reaction was performed in a DX.17MV Sequential stopped-flow ASVD spectrophotometer from Applied Photophysics (Leatherbarrow, England). Preparations to make the stopped-flow instrument anaerobic, using protocatechuic acid (PCA) and protocatechuate dioxygenase (PCD), were performed as described (*12*). The experiments were conducted at 25 °C at a constant ionic strength of 0.1. The CFeSP (7−8 μM) was reduced to cob(I)amide by incubation with 2 μM CODH/ACS and 1 μM FdII in 2 mM Tris-HCl, pH 7.6, under an atmosphere of carbon monoxide for 30 min. The resulting reduced CFeSP, containing 0.1 M NaCl, was rapidly mixed with 320 μM (6*RS*)-CH_3-H_4folate and 20.7 μM MeTr dimers in 50 mM MES buffers of the appropriate pH. The absorbance decrease at 390 nm, due to cob(I)amide depletion, and increase at 450 nm, due to methylcob(III)amide formation, was monitored in a cell with a path of 1 cm, and the stopped-flow traces were fit to a single-exponential equation using the software from Applied Photophysics. Other details are described in the legend to Figure 3A. The dissociation constant for the CFeSP−MeTr complex was measured also by single-turnover experiments, with the MeTr concentration varied at a constant (10 μM) CFeSP concentration, so that the absorbance changes due to methylation of cob(I)amide were identical for all traces. The CFeSP was reduced as described above and rapidly mixed at 25 °C with 200 μM (6*RS*)-CH_3-H_4folate and MeTr (5.2, 10, 20, 41, 82, and 124 μM, expressed as the dimeric unit) in 0.2 M MES, pH 5.1,

Scheme 1[a]

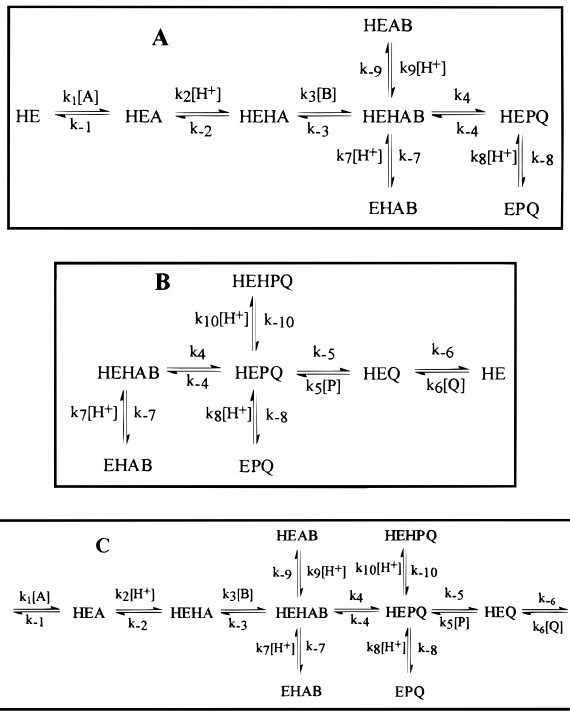

[a] A = CH_3-H_4folate; B = CFeSP; P = CH_3-CFeSP; Q = H_4folate; HExx = protonated active MeTr, Exx = unprotonated inactive MeTr.

2 mM DTT. The traces at 390 nm with a cell path of 1 cm were fit to single-exponential decay equations, and the average of 5−10 traces was plotted versus the final MeTr concentration as shown in Figure 2.

Simulation of Pre-Steady-State and Steady-State Traces. Pre-steady-state kinetic data obtained with CFeSP and CH_3-H_4folate at 25 °C and at different pH values were fitted by the program FITSIM (*26*) using the mechanism described in Scheme 1A. Similarly, the pre-steady-state kinetic data with CH_3-CFeSP and H_4folate were fitted using the mechanism shown in Scheme 1B. This allowed us to test the validity of the mechanism and to derive rate constants for steps that we could not determine experimentally. The resulting rate constants were then used to simulate the steady-state reaction progress curve with the KINSIM (*27*) program and to fit the rate constants by FITSIM using the mechanism shown in Scheme 1C. To allow an unrestrained evaluation of all parameters, the program was used in the steady-state mode, so that the equilibrium constants for individual steps were calculated from the fitted microscopic rate constants. Therefore, errors in individual equilibrium constants were calculated from the estimated errors on the fitted microscopic rate constants. The pH was set as a constant based on the concentrations of protonated and unprotonated MES buffer at each pH and the pK_a for the buffer (pK_a = 6.10). The rates for protonation of MES, free CH_3-H_4folate, and free H_4folate were all set to be diffusion-controlled (10^{10} M^{-1} s^{-1}), while the rates for deprotonation were calculated from the corresponding rates of protonation and the pK_a values. The pK_a values for free CH_3-H_4folate and H_4folate were set at 4.82 (*28*), while the pK_a values for bound CH_3-H_4folate and H_4folate were set at 5.80 (*20*). The default limits of FITSIM were used for all other rate constants (0 < zero-order rate constant < 10^{10} s^{-1}). The values of all final fitted rate constants were tested by repeating the FITSIM minimization using different initial estimates. The value of K_d for CFeSP was set at 8 μM, and the K_d for CH_3-H_4folate was set at 1.5 μM. Other details of the single-turnover and steady-state experiments are described in the legends of Figures 3 and 4, respectively.

RESULTS AND DISCUSSION

pH Dependence of the MeTr Reaction. The MeTr-catalyzed reaction is pH dependent. The pH dependencies for k_{cat}/K_m for each of the four substrates of MeTr (CFeSP, CH_3-H_4folate, CH_3-CFeSP, and H_4folate) increase as the pH is lowered with pK_a values ranging from 5.0 to 5.3 (with uncertainties of ∼0.1 pK unit in each case) [Table 1 in reference (*12*)]. If ionization of the substrate is rate-limiting, protonation of CH_3-H_4folate should increase the rate of the forward reaction, while protonation of H_4folate should decrease the rate of the reverse methyl transfer reaction. Furthermore, the pK_a of MeTr-bound CH_3-H_4folate is 5.80 (*20*), which differs significantly from the corresponding pK_a (5.10) for the k_{cat}/K_m for CH_3-H_4folate. These data strongly suggest that a rate-limiting ionization of MeTr, not of CH_3-H_4folate, is responsible for the pH dependence of the methyl transfer reaction. This hypothesis was consistent with fluorescence quenching studies that revealed a pH-dependent conformational change in MeTr with a characteristic pK_a of 5.0 ± 0.1 (*21*). It was proposed that at lower pH, the protein shifts to a conformation in which hydrophobic regions are exposed to solvent, favoring binding of the substrates CH_3-H_4folate and H_4folate to MeTr. However, the dissociation constant for CH_3-H_4folate from MeTr was, surprisingly, found to be pH independent (*20*). We hypothesize that the unprotonated substrate, the major form of CH_3-H_4folate in solution where MeTr is most active, is the preferred substrate, and upon binding to the enzyme, it undergoes protonation. Proton uptake experiments are consistent with this proposal (*20*).

To further test the concept that ionization of the enzyme leads to the observed pH dependence of the MeTr reaction, we performed the steady-state kinetic experiments shown in Figure 1. These experiments were performed by varying the [CFeSP] at saturating concentrations of (6*S*)-CH_3-H_4folate (K_d = 1.5 μM). Under these conditions, the apparent values of k_{cat} and k_{cat}/K_m correspond to the k_{cat} for the forward reaction and the k_{cat}/K_m for CFeSP, respectively. The pH dependence for k_{cat}/K_m for the CFeSP reproduces the pH profile previously obtained by steady-state first-order kinetics (*12*). Moreover, these results also show that the K_m for the CFeSP is pH independent between pH 4.9 and 7.6, which includes the physiological pH (∼6) and the region of maximum enzyme activity. The values of k_{cat} and k_{cat}/K_m are pH-dependent, with pK_a values of 5.6 and 5.1. Therefore, the binding of both substrates for the forward reaction is pH independent, and the pH dependence of this reaction must originate in ionizations occurring in the ternary complex, which affect k_{cat}. We propose that a similar behavior operates for the reverse methyl transfer, and our simulations (vide infra) are consistent with pH-independent binding of CH_3-CFeSP and H_4folate.

Initial Velocity and Product Inhibition Studies of CFeSP Methylation. Previous work established that transfer of the methyl group from CH_3-H_4folate to the CFeSP occurs by a direct S_N2-type mechanism (*12*). Thus, catalysis must occur

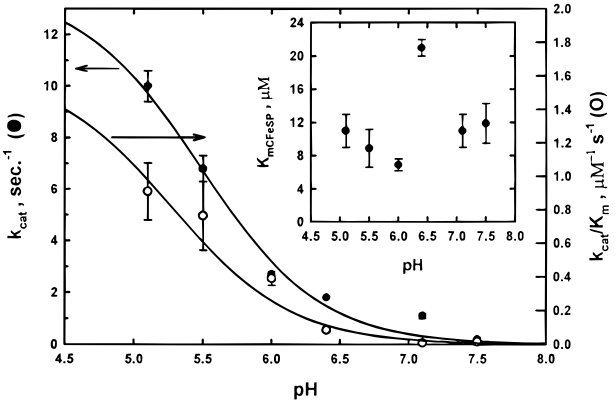

FIGURE 1: Dependence of k_{cat} and k_{cat}/K_m for CFeSP on pH. Initial rates were measured at 390 nm for the forward reaction of MeTr at 25 °C in 0.1 M MES at the appropriate pH and at an ionic strength of 0.1. The concentration of (6*RS*)-CH_3-H_4folate was held constant at 60 μM. The data at each pH were then fit to the Michaelis−Menten equation, yielding values of k_{cat} and K_m for the CFeSP. The pH dependence of k_{cat} for CFeSP was then fitted to a single ionization pH dependence, yielding values of $k_{cat} = 14.7 \pm 1.7$ s^{-1} and p$K_a = 5.43 \pm 0.11$. The same analysis for k_{cat}/K_m for CFeSP yielded $k_{cat}/K_m = 1.6 \pm 0.6$ μM^{-1} s^{-1} and p$K_a = 5.3 \pm 0.2$. Inset: Dependence of K_m for the CFeSP on the pH. The average K_m value is 12 ± 4 μM.

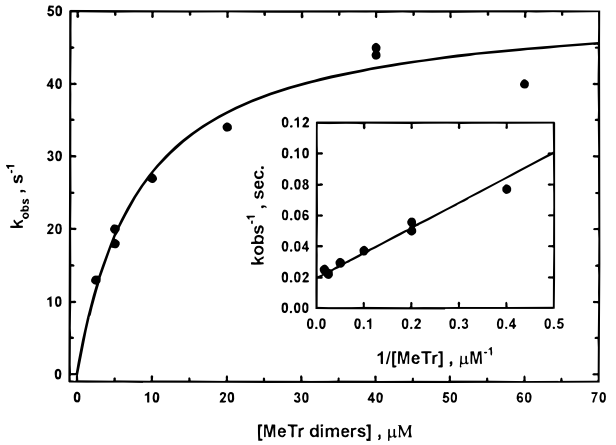

FIGURE 2: Dependence of the initial turnover rates on the MeTr concentration. CFeSP (10 μM initial concentration) was reduced as described under Materials and Methods and rapidly mixed with 100 μM (6*RS*)-CH_3-H_4folate and MeTr (as the dimer) at the following final concentrations: 5.2, 10, 20, 41, 82, and 124 μM in 0.2 M MES, pH 5.1, 2 mM DTT, at 25 °C. The traces at 390 nm with a cell path of 1 cm were fitted to single-exponential decay equations. Data are the average of at least 5 traces, and the curve is the fit to a saturation curve with $k_{max} = 50 \pm 3$ s^{-1} and $K_d = 8 \pm 1$ μM. Assuming p$K_a = 5.70$, the maximal value of k_{max} is 63 s^{-1}.

in a ternary complex. To obtain further evidence supporting (or otherwise) this mechanistic class and to determine if the reaction is ordered or random, we measured the dissociation constant for the CFeSP by single-turnover stopped-flow experiments (Figure 2). The value of the dissociation constant K_B is 8 μM, and the maximal rate constant is 50 s^{-1}. The general form of the type of steady-state kinetic mechanism is given in eq 2. The value of K_m for the CFeSP is very close to the K_B value. In addition, the K_m for CH_3-H_4folate determined previously equals the dissociation constant measured by fluorescence in the binary complex (*12*, *21*). Therefore, $K_B \approx \alpha K_B$ and $K_A \approx \alpha K_A$, and the CFeSP and CH_3-H_4folate must bind independently.

$$k_{obs} = \frac{k_{cat}}{[A][B] + \alpha K_A[B] + \alpha K_B[A] + \alpha K_A K_B} \quad (2)$$

To establish whether substrate binding is ordered or random, we performed product inhibition experiments. The results are summarized in Table 1. The product inhibition data were fitted to eq 3a with A (CH_3-H_4folate) varied and Q (H_4folate) as the inhibitor, eq 3b with A varied and P (CH_3-CFeSP) as the inhibitor, or eq 3c with B (CFeSP) varied and Q as the inhibitor:

$$\frac{1}{k_{obs}} = \frac{\alpha K_A}{k_{cat}}\left(1 + \frac{K_B}{[B]}\left(1 + \frac{[Q]}{K_Q}\right)\right)\frac{1}{[A]} + \frac{1}{k_{cat}}\left(1 + \frac{\alpha K_B}{[B]}\right) \quad (3a)$$

$$\frac{1}{k_{obs}} = \frac{\alpha K_A}{k_{cat}}\left(1 + \frac{K_B}{[B]}\left(1 + \frac{[P]}{K_P}\right)\right)\frac{1}{[A]} + \frac{1}{k_{cat}}\left(1 + \frac{\alpha K_B}{[B]}\right) \quad (3b)$$

$$\frac{1}{k_{obs}} = \frac{\alpha K_B}{k_{cat}}\left(1 + \frac{K_A}{[A]}\left(1 + \frac{[Q]}{K_Q}\right)\right)\frac{1}{[B]} + \frac{1}{k_{cat}}\left(1 + \frac{\alpha K_A}{[A]}\right) \quad (3c)$$

In these equations, K_A, K_B, K_P, and K_Q are the dissociation constants for CH_3-H_4folate, CFeSP, CH_3-CFeSP, and H_4-folate from free MeTr, respectively, and a value of $\alpha = 1.0$ (above) was assumed. With H_4folate as the product inhibitor at varying concentrations of (6*S*)-CH_3-H_4folate and constant unsaturating CFeSP concentrations, the lines in the double-reciprocal plots converge on the *y*-axis. This indicates competitive inhibition by H_4folate with respect to (6*S*)-CH_3-H_4folate ($K_Q = 16 \pm 6$ μM). When CH_3-CFeSP is used as the product inhibitor at varying (6*S*)-CH_3-H_4folate and constant unsaturating CFeSP, the lines in the double-reciprocal plots again converge on the *y*-axis, indicating that the CH_3-CFeSP is a competitive inhibitor with respect to CH_3-H_4folate ($K_P = 5.2 \pm 1.5$ μM). With H_4folate as the product inhibitor at varying CFeSP and constant unsaturating CH_3-H_4folate, H_4folate is a competitive inhibitor ($K_Q = 430 \pm 130$ μM) with respect to the CFeSP.[2] When H_4folate is used as the product inhibitor at varying concentrations of CFeSP and constant *saturating* CH_3-H_4folate concentrations, very slight product inhibition was observed ($K_Q = 1.3 \pm 0.8$ mM).[3] These four experiments, as shown by Table 1, rule out, from the common two-substrate reaction mecha-

[2] The equilibrium constant was calculated using k_{cat}/K_m for CFeSP (1.6 μM^{-1} s^{-1}), K_A for CH_3-H_4folate (1.5 μM), k_{cat}/K_m for CH_3CFeSP (60 s^{-1} divided by 95 μM), and K_Q for H_4folate (11 μM). The equilibrium constant is 14. Under conditions of high buffer concentration (50 mM), it is not necessary to include the contribution of the proton substrate.

[3] The experiments with H_4folate as the product inhibitor yielded two different values for its dissociation constant. With CH_3-H_4folate as substrate and the CFeSP concentration set at $2 \times K_B$, K_Q (16 ± 6 μM) agrees well with the independently estimated value from the simulations of steady-state traces (step 6 in Table 2, 11 μM). With CFeSP as a substrate and unsaturating (0.8 μM) or saturating CH_3-H_4folate (50 μM), the calculated values of K_Q are 460 ± 120 and 430 ± 380 μM, respectively. This could reflect two different binding modes of H_4-folate to MeTr. Indeed, fluorescence studies showed that CH_3-H_4folate binds to MeTr with two dissociation constants differing by 30-fold (1.5 and 50 μM) (20), which most likely reflect nonequivalent binding sites for CH_3-H_4folate. Similar behavior is observed for H_4folate. When the data are fit to a dual competitive inhibition model, K_Q values of 8 ± 3 and 850 ± 120 μM are obtained. The slight inhibition observed is presumably due to binding of H_4folate to the second binding site of MeTr. The value of K_P for CH_3-CFeSP agrees well with the simulated dissociation constant (step 5 in Table 2).

Table 1: Predicted Product Inhibition Patterns for Two Substrate Mechanisms[a]

mechanism	product inhibitors	varied substrate: (6*S*)-CH_3-H_4folate: unsaturated C/Fe-SP	(6*S*)-CH_3-H_4folate: saturated C/Fe-SP	C/Fe-SP: unsaturated CH_3-H_4folate	C/Fe-SP: saturated CH_3-H_4folate
ordered Bi-Bi	CH_3-C/Fe-SP	MT	UC	MT	MT
	H_4folate	C	C	MT	−
Theorell−Chance	CH_3-C/Fe-SP	MT	−	C	C
	H_4folate	C	C	MT	−
ping-pong	CH_3-C/Fe-SP	MT	−	C	C
	H_4folate	C	C	MT	−
rapid equilibrium	CH_3-C/Fe-SP	−	−	−	−
ordered Bi-Bi	H_4folate	C	−	C	−
random Bi-Bi	CH_3-C/Fe-SP	MT	MT	MT	MT
	H_4folate	MT	MT	MT	MT
rapid equilibrium	CH_3-C/Fe-SP	C	−	C	−
random Bi-Bi	H_4folate	C	−	C	−
rapid equilibrium					
random Bi-Bi	CH_3-C/Fe-SP	MT	−	C	C
with dead-end MeTr−CH_3-H_4folate−CH_3-C/Fe-SP	H_4folate	C	−	C	−
rapid equilibrium					
random Bi-Bi	CH_3-C/Fe-SP	C	−	C	−
with dead-end MeTr−C/Fe-SP-H_4folate	H_4folate	C	C	MT	−
our studies	CH_3-C/Fe-SP	C	nd	nd	nd
	H_4folate	C	nd	C	−

[a] Abbreviations: C, competitive; MT, mixed-type; UC, uncompetitive; nd, not determined; −, no inhibition.

nisms, all but the rapid equilibrium random Bi-Bi mechanism.[4] The product inhibition results further indicate that dead-end complexes, MeTr−CH_3-H_4folate−CH_3-CFeSP and MeTr−CFeSP−H_4folate, are not formed. Equations 3a−c, the velocity equations for the random Bi-Bi mechanism, gave good fits to the product inhibition data. These combined results are consistent with the mechanism shown in Scheme 2, in which the two substrates bind and form a ternary complex where catalysis occurs, and products randomly dissociate.

Pre-Steady-State Kinetic Measurements and Simulation of the MeTr Reaction. Steady-state kinetics can reveal the overall kinetic mechanism, but cannot identify the intermediates and the rates of elementary reaction steps. Pre-steady-state kinetic experiments can identify intermediates and allow direct measurement of the rate constants for most of the steps. Solution of the entire kinetic mechanism requires integration of all the steady-state and pre-steady-state kinetic data by simulating the reaction progress curve. This final step is important because the cell operates primarily under steady-state conditions.

We performed single-turnover stopped-flow experiments at different pH values in the forward direction, following the decay of the cob(I)amide form of the CFeSP ($\lambda = 390$ nm), and in the reverse direction, following the decay of the methylcob(III)amide state ($\lambda = 450$ nm). After fitting each data set to a single-exponential decay equation and plotting the average rate constant at each pH, we obtained values for the maximal rate constants and pK_a values that reproduce the pre-steady-state values determined by a previous stopped-flow study (Figures 4 and 6 in reference *12*). We then simulated the single-turnover traces with the programs FITSIM and KINSIM (Figure 3) using the mechanisms shown in Schemes 1A (for the forward reaction) and 1B (for the reverse reaction). In these schemes, acid−base ionizations are included in the ternary complexes (steps 7 and 8 in Table 2). These results suggest that a pH-dependent protein conformational change in the ternary complex is linked to deprotonation of the active complexes HEHAB and HEPQ. This leads to formation of the dead-end inactive EHAB and EPQ complexes. This conformational change in the free enzyme (depicted in Scheme 2) was previously observed by fluorescence studies. The work described here suggests that substrate binding slightly elevates the pK_a for this confor-

Scheme 2

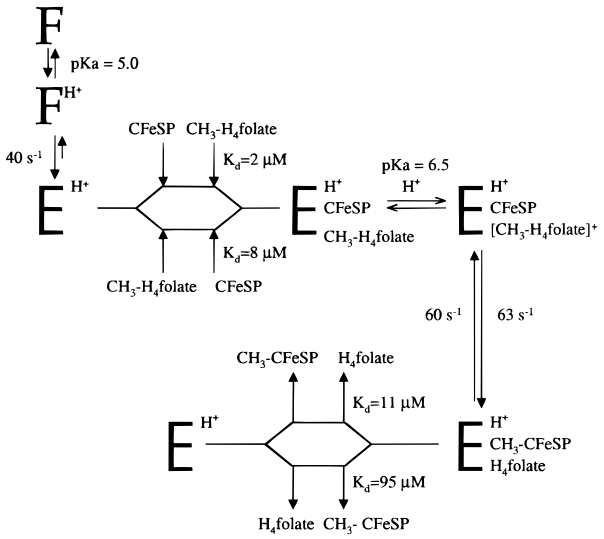

[4] There are four additional combinations of substrate and product inhibitors; however, these would have been extremely difficult experiments to perform. Since the K_m value for the CFeSP is 10 μM, performing product inhibition experiments at saturating concentrations of CFeSP would have required ~100 μM protein in each reaction mixture. Even if we achieved this technically difficult task, there would have been a huge background absorbance. Similarly, using CH_3-CFeSP as a product inhibitor at high concentrations is difficult because its overlapping absorbance at 390 nm would have dwarfed the relatively small absorbance changes of the reaction. However, sufficient data were collected to rule out all but one of the common two-substrate mechanisms, which strongly suggests that the reaction follows a random Bi-Bi mechanism.

Table 2: Summary of Microscopic Rate Constants for the MeTr Mechanism

process step no.	CH_3-H_4folate binding 1	H^+ binding 2	CFeSP binding 3	methyl transfer 4	CH_3-CFeSP binding 5	H_4folate binding 6	EHAB + H^+ kinetic pK_a 7	EPQ + H^+ kinetic pK_a 8	HEAB + H^+ amplitude pK_a 9	HEPQ + H^+ amplitude pK_a 10
k_{on} (μM^{-1} s^{-1})[a]	11[b]	650 ± 600	2.74 ± 0.05	63 s^{-1}	8.3 ± 4.0[d]	15 ± 13	9.5 ± 0.8	600 ± 300	1300 ± 1300	64 ± 40
k_{off} (s^{-1})	16	1500 ± 1500	22.0 + 0.4[c]	60 ± 2	34 ± 15[d]	1.4 ± 0.3	98 ± 8	1600 ± 800	400 ± 400	60 ± 40
K_d (μM)	1.5	2.3 ± 3.1	8		4.1 ± 2.6	11 ± 9	10.3 ± 1.2	2.7 ± 1.9	0.31 ± 0.44	0.94 ± 0.80
pK constant		5.7 ± 0.6					5.00 ± 0.05	5.6 ± 0.3	6.5 ± 0.6	6.0 ± 0.4

[a] All second-order rate constants are given as μM^{-1} s^{-1}, the maximum limit was set at 1000 μM^{-1} s^{-1}. [b] Underlined values were set constant during the simulations. For CH_3-H_4folate, K_A was set at 1.5 μM. [c] For CFeSP, K_B was set at 8 μM while k_3 was simulated. [d] Values of k_5 and k_{-5} are the average of the rate constants obtained from simulation of the steady-state for the forward direction data shown in Figure 4A,B.

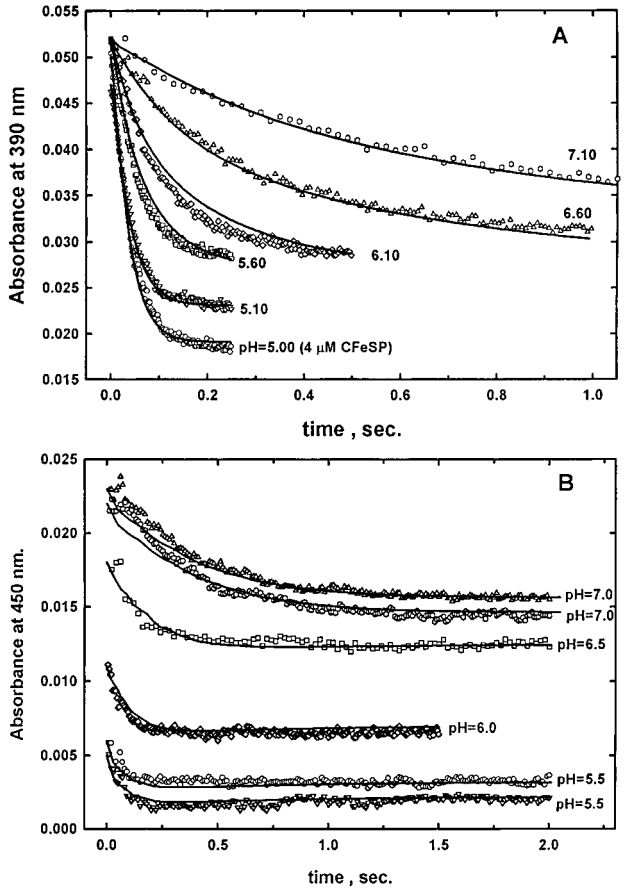

FIGURE 3: (A) Simulation of MeTr single-turnover forward reaction. Traces at the indicated pH values were obtained by rapidly mixing 20.7 μM MeTr monomers and 160 μM (6*RS*)-CH_3-H_4folate (final concentrations) with 3.0 μM reduced CFeSP (trace at pH 5.0 has 4.0 μM CFeSP final concentration) in 50 mM MES, ionic strength of 0.1 at 25 °C. Fits correspond to the simulations to the partial mechanism shown in Scheme 1A with the rate constants shown in Table 2. An extinction coefficient for the reaction is 0.017 OD μM^{-1} at 390 nm. (B) Simulation of MeTr single-turnover reverse reaction. Traces were obtained by rapidly mixing 20 μM MeTr and 100 μM H_4folate with 10.0 μM CH_3-CFeSP in 50 mM MES, ionic strength of 0.1 at 25 °C. The curves are fits to simulations of the mechanism shown in Scheme 1B using the rate constants in Table 2. The extinction coefficient at 450 nm was 0.006 OD μM^{-1}.

mational change, which would enhance the reactivity of the enzyme, since it is the protonated form that is most active. The amplitudes of the forward and reverse reactions (not shown), which reflect the amount of cob(I)amide and methylcob(III)amide formed during the reaction, are pH dependent. The amplitudes of the forward reaction decrease and those of the reverse direction increase with increasing pH. These dependencies are consistent with protonation of *bound* CH_3-H_4folate (HEAB) in the forward direction (HEAB + H^+ → HEHAB), and deprotonation of bound H_4folate (HEHPQ → HEPQ + H^+) in the reverse direction.

Our results indicate that the unprotonated form of CH_3-H_4folate (A) binds MeTr and then undergoes protonation in the ternary complex. First, if the protonated form (HA) were the substrate, a strong pH dependence of K_A would be expected. In contrast, K_a is pH independent. Second, the k_{cat}/K_m for CH_3-H_4folate matches the pK_a of the MeTr conformational change, not the pK_a of the free substrate. Third, the unprotonated form of CH_3-H_4folate is the predominant form at pH values higher than 5.0 (>60%). We fitted the forward single-turnover traces using a fixed value for K_A = 1.5 μM, as determined by fluorescence quenching, and fixed values of K_B = 8 μM and k_{max} = 50 s^{-1}, as determined from single-turnover experiments at pH 5.1 (Figure 2), and both were assumed to be pH independent. The maximal forward rate constant (k_4 = 63 s^{-1}) was calculated from the value of k_{max} after extrapolation to limiting low pH using a previously established pK_a value of 5.8 (Figure 4 and Table 1 in reference *12*). A similar mechanism (shown by Scheme 1B) was used for the reverse reaction. From these two sets of experiments, we derived the following rate constants: binding and release of CFeSP (k_3 = 2.7 μM^{-1} s^{-1} and k_{-3} = 22 s^{-1}, respectively); reverse methyl transfer (k_{-4} = 60 s^{-1}); and proton binding and release for the complexes EHAB (k_7 and k_{-7}, respectively) and EPQ (k_8 and k_{-8}). The resulting fitted rate constants are given in Table 2. The rate constants for the pH-dependent amplitude changes could not be estimated by using FITSIM (k_9 through k_{-10}), presumably because they constitute dead-end complexes in the mechanism, but the pK_a values for HEHAB and HEHPQ are around 6.5 and 6.0, respectively.

The rate constants obtained from single-turnover experiments were then used to simulate and fit the steady-state traces. To simplify the simulation of the steady-state traces, a mechanism with only one of the branches of the random mechanism was used, as shown by Scheme 1C. This does not alter any of the derived rate constants, since the substrates and products bind and dissociate independently. Traces at several pH values under k_{cat} conditions (74 μM CFeSP, 70 μM CH_3-H_4folate, and 108 nM MeTr monomers) were used in the simulation. From the corresponding simulations, we could derive the rate constants for binding and release of methylated CFeSP and H_4folate (k_5, k_{-5}, k_6, and k_{-6}) and for the proton required for the forward reaction. The results are tabulated in Table 2.

Overall MeTr Mechanism. Based on the combined results described above, we propose the following catalytic mechanism for MeTr (Scheme 2). The first, which could be considered to occur prior to the catalytic cycle, is a

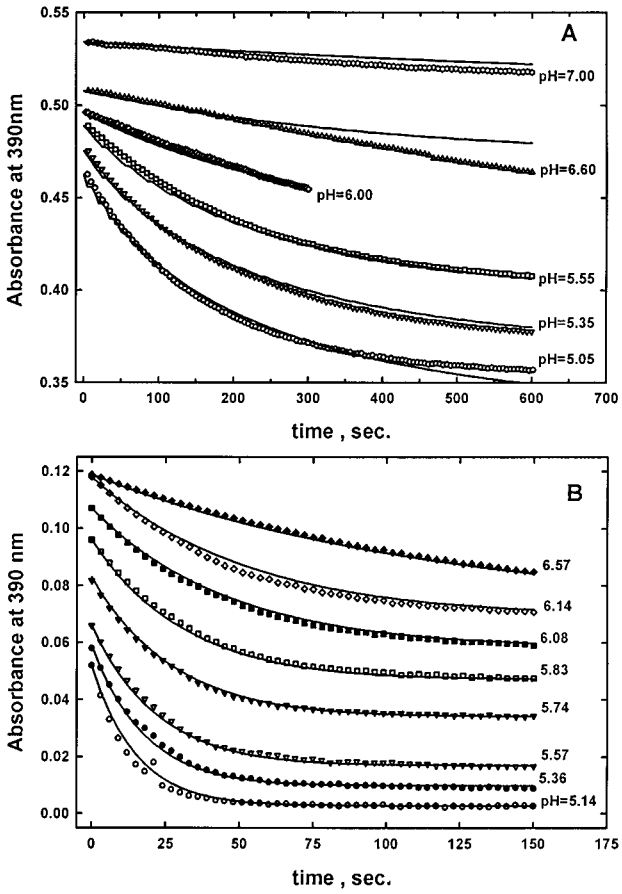

FIGURE 4: (A) Simulation of the forward MeTr reaction at saturating conditions. The experimental data were obtained by following the methylation of the CFeSP by CH_3-H_4folate (shown in symbols). The reaction consisted of 62 nM MeTr monomers, 74 μM CFeSP, and 70 μM (6*RS*)-CH_3-H_4folate in 50 mM MES at the appropriate pH, ionic strength 0.1 at 25 °C. The absorbance decrease at 390 nm ($\Delta\epsilon = 0.0034$ OD μM^{-1}) was monitored. The data are offset for clarity. Curves are fits to the mechanism shown in Scheme 1C with the rate constants shown in Table 2. (B) Simulation of the forward MeTr reaction at k_{cat}/K_m for CFeSP conditions. The reaction mixture contained 2.9 μM CFeSP, 120 μM CH_3-H_4folate, 2.1 mM titanium(III) citrate, and 108 nM MeTr in 800 μL of 50 mM MES buffer ($I = 0.1$) at various pH values as shown. The reaction was followed to completion at 25 °C, and the absorbance decrease at 390 nm was monitored. The data were plotted using offset values of 0.25, 0.31, 0.24, 0.22, 0.24, 0.22, 0.16, and 0.18 for pH 5.14, 5.36, 5.57, 5.74, 5.83, 6.08, 6.4, and 6.57, respectively. Curves are fits to the mechanism shown in Scheme 1C and rate constants shown in Table 2.

pH-dependent conformational change of the protein. This step rationalizes the pH dependencies of all the first-order kinetic parameters and the pH independence of the dissociation constants and the Michaelis constants for CFeSP and CH_3-H_4folate. The conformational change does not occur at each cycle of catalysis, but is an activation/deactivation phenomenon. In the present set of experiments, we observe the conformational change as dead-end ionizations of the complexes HEHAB and HEPQ, with a pK_a between 5.0 and 5.7. Previous fluorescence studies of the pH-dependent conformational change were performed with the free enzyme and indicated a pK_a of 5.0 (*12*). These ionizations are not rate-limiting as previously proposed (*12*), but are essential for the increased activity of the enzyme at low pH.

The catalytic cycle begins with substrate binding. MeTr binds CH_3-H_4folate and the CFeSP in a completely random manner. The product inhibition studies rule out all possible mechanisms but the random Bi-Bi mechanism. This is not a rapid equilibrium mechanism since k_3 (Table 2) is rate-limiting under k_{cat}/K_m conditions for the CFeSP and k_1 is rate-limiting under k_{cat}/K_m conditions for CH_3-H_4folate. There are some striking mechanistic differences between MeTr and methionine synthase. In this enzyme, methylcobalamin is a tightly bound prosthetic group, and its substrates bind by an ordered mechanism, with CH_3-H_4folate binding first, followed by homocysteine (*29*). The methyl transfer step and the overall forward reaction occur at similar rates in MeTr and methionine synthase; however, the methyl transfer step and the overall reaction of methionine formation are irreversible in methionine synthase. Several *S*-adenosyl-L-methionine-dependent methyltransferases follow Bi-Bi random mechanisms including the methyltransferase from *Euglena gracilis* (*30*), the DNA methyltransferase from bovine thymus (*31*), catechol-*O*-methyltransferase (*32*), L-isoaspartyl-D-aspartyl protein-*O*-carboxymethyl transferase (*33*), and *S*-adenosyl-L-methionine glutamylmethyl transferase from *Salmonella typhimurium* (*34*).

An important result of our studies and those described in the accompanying paper (*20*) is that protonation of CH_3-H_4folate is a key step in the MeTr reaction mechanism. This step has been proposed based on chemical principles (*18*). Chemical modeling studies also indicate that quaternization of the N^5 group by protonation or electrophilic coordination can activate CH_3-H_4folate (*35*, *36*). The pH dependence of the amplitudes for the forward and reverse reactions of MeTr constitutes the first experimental evidence that this protonation reaction occurs in a methyltransferase. Some of the error limits are relatively high, because the simulations are global analyses that include multiple data sets collected at pH values between 5 and 7. However, the exact pK_a value is not so important. The important conclusion is that an ionization in the ternary complex with a pK_a of around 6.0 is required to give satisfactory fits to all the data over this pH range. These pK_a values yielded by the simulations also are in complete agreement with the pK_a values previously determined by steady-state and transient kinetics (*12*). In the accompanying paper, it is shown that a proton is taken up as CH_3-H_4folate binds MeTr and that the pK_a for bound CH_3-H_4folate is 1 pH unit higher than that for free substrate (*20*). This proton transfer step must occur much faster than the transmethylation step, which is primarily rate determining for the overall reaction. This is consistent with the absence of a solvent isotope effect on the pre-steady-state reaction (*12*). If the rate constants for protonation (k_2) and deprotonation (k_{-2}) for the binary complex in Scheme 1A are constrained with a pK_a value of 5.80, which gives a K_d for the proton of 1.60 μM, the protonation rate constant (k_2 in Table 2) is 45 ± 5 μM^{-1} s^{-1}. The corresponding pK_a value for the amplitude for the ternary complex HEHAB is 6.5, which indicates that binding of CFeSP to HEHA further increases the pK_a of MeTr-bound CH_3-H_4folate. Protonation of H_4folate inhibits the reverse reaction, but the binding of CH_3-CFeSP to HEQ does not significantly perturb the pK_a of MeTr-bound H_4folate, which is around 5.80 (*20*).

The dissociation constant for H_4folate, obtained by simulations ($K_Q = 11$ μM) and product inhibition studies ($K_Q = 16 \pm 6$ μM), is higher than that for CH_3-H_4folate, as estimated from simulations ($K_A = 1.5$ μM) and fluorescence

measurements (*20*). Using the Haldane equation for the random mechanism,[2] we obtain an equilibrium constant for the overall reaction of 14. These results also indicate that MeTr preferentially catalyzes the forward methylation of CFeSP over the reverse reaction.

The products of the reaction rapidly dissociate from MeTr to close the catalytic cycle. When CH_3-CFeSP dissociates from MeTr, it interacts with and donates its methyl group to CODH/ACS for the final steps in the Wood−Ljungdahl pathway. The NiFeS cluster at the ACS active site must have access to the same upper face of the cobamide cofactor (that earlier interacted with CH_3-H_4folate) to perform a nucleophilic attack on the methylcobalt species. There is evidence that the FeS cluster in the CFeSP interacts with the CODH component and that the Co center interacts with the ACS component of the CODH/ACS bifunctional protein (*10*). In methanogens, a complex of five proteins appears to be required to convert acetyl-CoA to a methyl-pterin, carbon monoxide, and CoA (the reverse of acetyl-CoA synthesis) (*37*−*39*). In *C. thermoaceticum*, these proteins separate easily during the early steps of protein purification; however, it is likely that the CFeSP, MeTr, and CODH occur in a supermolecular complex in the cell. Clearly, methylation and demethylation of the CFeSP must be finely orchestrated so that CH_3-H_4folate and MeTr bind the cob(I)amide form of CFeSP and that CODH/ACS binds the methylated CFeSP after MeTr has dissociated.

CONCLUSIONS

The major findings of the present study are the following:

The MeTr reaction follows a random order kinetic mechanism.

The rate-limiting step in the forward and reverse directions under k_{cat} conditions is the methyl transfer step. Under k_{cat}/K_m conditions for each substrate, binding of that substrate is rate limiting.

The pH-dependent protein conformational change, which interconverts active and inactive states of the protein, is not a rate-limiting step or required for each cycle of catalysis.

The amplitude for single-turnover experiments in the forward and reverse directions reflects the protonation of the pterin ring of CH_3-H_4folate and H_4folate when bound to MeTr. This generates a positive charge at the N^5 position, which enhances the electrophilicity of the methyl group, thus activating it for nucleophilic attack by cob(I)amide.

ACKNOWLEDGMENT

We thank Professor Bryce Plapp (Department of Biochemistry, University of Iowa) for providing us with KINSIM and FITSIM programs and for his advice on data fitting.

REFERENCES

1. Ljungdahl, L. G. (1986) *Annu. Rev. Microbiol. 40*, 415−450.
2. Ragsdale, S. W. (1991) *CRC Crit. Rev. Biochem. Mol. Biol. 26*, 261−300.
3. Ragsdale, S. W., and Kumar, M. (1996) *Chem. Rev. 96*, 2515−2539.
4. Drake, H. L., Hu, S.-I., and Wood, H. G. (1981) *J. Biol. Chem. 256*, 11137−11144.
5. Doukov, T., Zhao, S., Roberts, D. L., Kim, J.-J., Ragsdale, S. W., and Stezowski, J. (1995) *Acta Crystallogr., D51: Part 6*, 1092−1093.
6. Roberts, D. L., Zhao, S., Doukov, T., and Ragsdale, S. W. (1994) *J. Bacteriol. 176*, 6127−6130.
7. Roberts, D. L., James-Hagstrom, J. E., Smith, D. K., Gorst, C. M., Runquist, J. A., Baur, J. R., Haase, F. C., and Ragsdale, S. W. (1989) *Proc. Natl. Acad. Sci. U.S.A. 86*, 32−36.
8. Hu, S.-I., Pezacka, E., and Wood, H. G. (1984) *J. Biol. Chem. 259*, 8892−8897.
9. Ragsdale, S. W., Lindahl, P. A., and Münck, E. (1987) *J. Biol. Chem. 262*, 14289−14297.
10. Menon, S., and Ragsdale, S. W. (1998) *Biochemistry 37*, 5689−5698.
11. Lu, W.-P., Schiau, I., Cunningham, J. R., and Ragsdale, S. W. (1993) *J. Biol. Chem. 268*, 5605−5614.
12. Zhao, S., Roberts, D. L., and Ragsdale, S. W. (1995) *Biochemistry 34*, 15075−15083.
13. Menon, S., and Ragsdale, S. W. (1999) *J. Biol. Chem.* (in press).
14. Jarrett, J. T., Amaratunga, M., Drennan, C. L., Scholten, J. D., Sands, R. H., Ludwig, M. L., and Matthews, R. G. (1996) *Biochemistry 35*, 2464−2475.
15. Harder, S. A., Lu, W.-P., Feinberg, B. F., and Ragsdale, S. W. (1989) *Biochemistry 28*, 9080−9087.
16. Wirt, M. D., Kumar, M., Ragsdale, S. W., and Chance, M. R. (1993) *J. Am. Chem. Soc. 115*, 2146−2150.
17. Wirt, M. D., Wu, J.-J., Scheuring, E. M., Kumar, M., Ragsdale, S. W., and Chance, M. R. (1995) *Biochemistry 34*, 5269−5273.
18. Matthews, R. G., Banerjee, R. V., and Ragsdale, S. W. (1990) *BioFactors 2*, 147−152.
19. Matthews, R. G. (1999) in *Vitamin B_{12}* (Banerjee, R., Ed.) Vol. 1, Chapter 15, John Wiley and Sons, New York (in press).
20. Seravalli, J., Shoemaker, R. K., Sudbeck, M. J., and Ragsdale, S. W. *Biochemistry*, (1999) *Biochemistry 38*, 5736−5745.
21. Zhao, S. Y., and Ragsdale, S. W. (1996) *Biochemistry 35*, 2476−2481.
22. Andreesen, J. R., Schaupp, A., Neurater, C., Brown, A., and Ljungdahl, L. G. (1973) *J. Bacteriol. 114*, 743−751.
23. Elliott, J. I., and Ljungdahl, L. G. (1982) *J. Bacteriol. 151*, 328−333.
24. Ragsdale, S. W., Ljungdahl, L. G., and DerVartanian, D. V. (1983) *J. Bacteriol. 155*, 1224−1237.
25. Elliott, J. I., and Brewer, J. M. (1978) *Arch. Biochem. Biophys. 190*, 351−357.
26. Zimmerle, C. T., and Frieden, C. (1989) *Biochem. J. 258*, 381−387.
27. Barshop, B. A., Wrenn, R. F., and Frieden, C. (1983) *Anal. Biochem. 133*, 134−145.
28. Kallen, R. G., and Jencks, W. P. (1966) *J. Biol. Chem. 241*, 5845−5850.
29. Banerjee, R., Frasca, V., Ballou, D. P., and Matthews, R. G. (1990) *Biochemistry 29*, 11101−11109.
30. Hinchigeri, S. B., and Richards, W. R. (1982) *Photosynthetica 16*, 554−560.
31. Sano, H., Noguchi, H., and Sager, R. (1983) *Eur. J. Biochem 135*, 181−185.
32. Coward, J. K., Slisz, E. P., and Wu, F. Y.-H. (1973) *Biochemistry 12*, 2291−2297.
33. Jamaluddin, S., Kim, S., and Paik, W. K. (1975) *Biochemistry 14*, 694−698.
34. Simon, A. S., and Subbaramaiah, K. (1991) *J. Biol. Chem. 266*, 12741−12745.
35. Hilhorst, E., Iskander, A. S., Chen, T. B. R. A., and Pandit, U. (1993) *Tetrahedron Lett. 34*, 4257−4260.
36. Hilhorst, E., Iskander, A. S., Chen, T. B. R. A., and Pandit, U. (1994) *Tetrahedron 50*, 8863−8870.
37. Abbanat, D. R., and Ferry, J. G. (1990) *J. Bacteriol. 172*, 7145−7150.
38. Grahame, D. A. (1991) *J. Biol. Chem. 266*, 22227−22233.
39. Grahame, D. A., and Demoll, E. (1996) *J. Biol. Chem. 271*, 8352−8358.

BI982473C